Sains Malaysiana 41(12)(2012): 1643–1649

Mixed Convection Flow about a Solid Sphere Embedded in a Porous Medium Filled with a Nanofluid

(Aliran Olakan Campuran terhadap Sfera Pejal yang Terbenam dalam Medium Berliang dengan Nanobendalir)

LEONY THAM & ROSLINDA NAZAR*

ABSTRACT

A steady laminar mixed convection boundary layer flow about an isothermal solid sphere embedded in a porous medium filled with a nanofluid has been studied for both cases of assisting and opposing flows. The transformed boundary layer equations were solved numerically using an implicit finite-difference scheme. Three different types of nanoparticles, namely Cu, Al_2O_3 and TiO_2 in water-based fluid were considered. Numerical solutions were obtained for the skin friction coefficient, the velocity and temperature profiles. The features of the flow and heat transfer characteristics for various values of the nanoparticle volume fraction and the mixed convection parameters were analyzed and discussed.

Keywords: Boundary layer; mixed convection; nanofluid; porous medium; solid sphere

ABSTRAK

Aliran lapisan sempadan olakan campuran berlamina mantap terhadap sfera pejal isoterma yang terbenam dalam medium berliang dengan nanobendalir telah dikaji bagi kes aliran membantu dan aliran menentang. Persamaan lapisan sempadan terjelma diselesaikan secara berangka dengan skema beza terhingga tersirat. Tiga jenis nanozarah dalam bendalir asas air dipertimbangkan, iaitu Cu, Al_2O_3 and TiO_2. Penyelesaian berangka diperoleh bagi pekali geseran kulit, profil halaju dan profil suhu. Ciri-ciri aliran dan pemindahan haba bagi pelbagai nilai parameter pecahan isi padu nanozarah dan parameter olakan campuran dianalisis dan dibincangkan.

Kata kunci: Lapisan sempadan; medium berliang; nanobendalir; olakan campuran; sfera pejal

INTRODUCTION

The convective heat transfer in a fluid saturated porous media have considerable applications in mechanical, chemical and civil engineering, including fibrous insulation, food processing and storage, thermal insulation of buildings, geophysical systems, the design of pebble bed nuclear reactors, underground disposal of nuclear waste, solar power collectors, geothermal applications and nuclear reactors (Nield & Bejan 2006). Due to the fact that conventional heat transfer fluids such as oil, water and ethylene glycol mixture are less productive in transferring the heat, the thermal conductivity by fluid flow, that is, the heat transfer coefficient between the heat transfer medium and the heat transfer surface can be improved by using nanofluids. Heat transfer by nanofluids is an innovative technique for improving heat transfer by using ultra fine solid particles in the fluids. The term nanofluid was firstly used by Choi (1995) to define the dilution of nanometer-sized particles (smaller than 100 nm, such as metals oxides, carbides or carbon nanotubes) in a fluid (water, ethylene glycol and oil). These nanofluids have better thermal conductivity and convective heat transfer coefficient compared with the base fluid only, because of the diluted nanometer-sized nanoparticles that can easily flow smoothly through the microchannels (Khanafer et al. 2003) and as such, nanofluids are widely used as coolants, lubricants and heat exchangers.

The utility of a particular nanofluid for a heat transfer application can be established by suitably modeling the convective transport in the nanofluid (Kumar et al. 2010). Numerical and experimental studies on nanofluids have been performed, including the study on thermal conductivity (Kang et al. 2006), separated flow (Abu-Nada 2008) and convective heat transfer (Jou & Tzeng 2006). Daungthongsuk and Wongwises (2008) studied the influence of the thermophysical properties of nanofluids on the convective heat transfer and summarized various models used in the literature for predicting the thermophysical properties of nanofluids. Eastman et al. (2010) used pure copper nanoparticles of less than 10 nm in size and achieved a 40% increase in thermal conductivity for only 0.3% volume fraction of the solid dispersed in ethylene glycol. Further references on nanofluids can be found in Das et al. (2007) and in the review paper by Buongiorno (2006). There are several published papers on nanofluids that have used the Buongiorno nanofluid model.

However, in this paper, we will use the nanofluid model proposed by Tiwari and Das (2007) to study the present problem of mixed convection boundary layer flow

about a solid sphere embedded in a porous medium filled with a nanofluid. On the other hand, Nazar et al. (2011) have considered the mixed convection boundary layer flow from a horizontal circular cylinder embedded in a porous medium filled with a nanofluid by extending the papers by Ahmad and Pop (2010), Cheng (1982), Merkin (1977) and Nazar et al. (2003). It is worth to point out that this nanofluid model was very successfully used by Abu-Nada (2008), Arifin et al. (2011), Abu-Nada and Oztop (2009), Bachok et al. (2010), Oztop and Abu-Nada (2008) and Rosca et al. (2012).

Basic Equations

Consider the steady mixed convection boundary layer flow about an impermeable solid sphere of radius a embedded in a porous medium filled with a nanofluid. It is assumed that the constant temperature of the surface of the sphere is T_w, while the constant ambient temperature value is T_∞, where $T_w > T_\infty$ for a heated sphere (assisting flow) and $T_w < T_\infty$ for a cooled sphere (opposing flow). It is also assumed that the velocity of the external flow (inviscisd flow) or the local free stream velocity is $u_e(x)$, where x is the coordinate measured along the surface of the sphere starting from the lower stagnation point. The Boussinesq approximation is employed and the homogeneity and local thermal equilibrium in the porous medium are assumed. It is also assumed that the nanoparticles are suspended in the nanofluid using either surfactant or surface charge technology. In keeping with the Darcy law and adopting the nanofluid model proposed by Tiwari and Das (2007), we obtain the following boundary layer equations for the problem under consideration in dimensionless form as:

$$\frac{\partial(ru)}{\partial x} + \frac{\partial(rv)}{\partial y} = 0, \tag{1}$$

$$\frac{1}{(1-\varphi)^{2.5}}\frac{\partial u}{\partial y} = \left[(1-\varphi) + \varphi\left(\rho_s/\rho_f\right)\left(\beta_s/\beta_f\right)\right]\frac{\partial \theta}{\partial y}\lambda \sin x, \tag{2}$$

$$u\frac{\partial \theta}{\partial x} + v\frac{\partial \theta}{\partial y} = \frac{\alpha_{nf}}{\alpha_f}\frac{\partial^2 \theta}{\partial y^2}, \tag{3}$$

subject to the boundary conditions

$$\begin{aligned} &v(x, y) = 0,\ \theta(x, y) = 1 \quad \text{at} \quad y = 0,\ 0 \le x \le \pi, \\ &u(x, y) \to u_e(x) = \frac{3}{2}\sin x, \\ &\theta(x, y) \to 0 \quad \text{as} \quad y \to \infty,\ 0 \le x \le \pi. \end{aligned} \tag{4}$$

Here u and v are the velocity components along the x and y axes, respectively, $r(x)$ is the radial distance from the symmetrical axis to the surface of the sphere, $u_e(x)$ is the local free stream velocity, T is the fluid temperature, φ is the solid volume fraction of the nanofluid or the nanofluid volume fraction, β_f is the thermal expansion coefficient of the fluid fraction, β_s is the thermal expansion coefficient of the solid fraction, α_{nf} is the thermal diffusivity of the nanofluid, ρ_f and ρ_s are the density of the fluid and solid fractions, respectively, μ_{nf} is the viscosity of the nanofluid and g is the magnitude of the gravity acceleration, which are given by (Oztop & Abu-Nada 2008):

$$\begin{aligned} &\mu_{\mathrm{nf}} = \frac{\mu_{\mathrm{f}}}{(1-\varphi)^{2.5}},\ (\rho C_p)_{\mathrm{nf}} = (1-\varphi)(\rho C_p) + \varphi(\rho C_p)_s, \\ &\alpha_{\mathrm{nf}} = \frac{k_{\mathrm{nf}}}{(\rho C_p)_{nf}},\ \frac{k_{\mathrm{nf}}}{k_{\mathrm{f}}} = \frac{(k_{\mathrm{s}} + 2k_{\mathrm{f}}) - 2\varphi(k_{\mathrm{f}} - k_{\mathrm{s}})}{(k_{\mathrm{s}} + 2k_{\mathrm{f}}) + \varphi(k_{\mathrm{f}} - k_{\mathrm{s}})}, \end{aligned} \tag{5}$$

where k_{nf} is the effective thermal conductivity of the nanofluid, k_f is the thermal conductivity of the fluid, k_s is the thermal conductivity of the solid, $(\rho C_p)_{nf}$ is the heat capacity of the nanofluid, $(\rho C_p)_f$ is the heat capacity of the fluid and $(\rho C_p)_s$ is the heat capacity of the solid. The flow is assumed to be slow so that an advective term and a Forchheimer quadratic drag term do not appear in the Darcy equation (2). The viscosity of the nanofluid can be approximated as the viscosity of the base fluid containing the diluted suspension of fine spherical particles and is given by Brinkman (1952).

Here λ is the mixed convection parameter, which are defined as $\lambda = Ra/Pe$, with $Ra = gK\beta(T_w - T_\infty)\ a\ /\ \nu_f\alpha_f$, being the modified Rayleigh number for the porous medium. It is worth mentioning that $\lambda > 0$ for an assisting flow ($T_w > T_\infty$), $\lambda < 0$ for an opposing flow ($T_w < T_\infty$) and $\lambda = 0$ for the forced convection flow. Integrating Equation (2) and using the boundary conditions (4), we obtain:

$$\begin{aligned} \frac{1}{(1-\varphi)^{2.5}}u = \frac{3}{2}\frac{\sin x}{(1-\varphi)^{2.5}} \\ + \left[(1-\varphi) + \varphi\left(\rho_s/\rho_f\right)\left(\beta_s/\beta_f\right)\right]\lambda\theta \sin x. \end{aligned} \tag{6}$$

In order to solve (1), (3) and (6), subject to the boundary conditions (4), we assumed the following variables:

$$\psi = xr(x)\, f(x, y),\ \theta = \theta(x, y), \tag{7}$$

where ψ is the stream function, which is defined in the usual way as $u = (1/r)\ \partial\psi/\partial y$ and $v = -(1/r)\partial\psi/\partial x$, that automatically satisfies Equation (1).

Substituting the variables (7) into (3) and (6), and after some algebra, we obtain the following transformed equations:

$$\frac{1}{(1-\varphi)^{2.5}}\frac{\partial f}{\partial y} = \left\{\begin{aligned} &\frac{3}{2}\frac{1}{(1-\varphi)^{2.5}} + \\ &\left[(1-\varphi) + \varphi\left(\rho_s/\rho_f\right)\left(\beta_s/\beta_f\right)\right]\lambda\theta \end{aligned}\right\}\frac{\sin x}{x}, \tag{8}$$

$$\begin{aligned} \frac{k_{nf}/k_f}{(1-\varphi) + \varphi\left(\rho C_p\right)_s/\left(\rho C_p\right)_f}\frac{\partial^2 \theta}{\partial y^2} + f\frac{\partial \theta}{\partial y} \\ = x\left(\frac{\partial f}{\partial y}\frac{\partial \theta}{\partial x} - \frac{\partial f}{\partial x}\frac{\partial \theta}{\partial y}\right), \end{aligned} \tag{9}$$

with the boundary conditions:

$$f(x, y) = 0,\ \theta(x, y) = 1 \quad \text{at } y = 0, \quad 0 \le x \le \pi,$$

$$\frac{\partial f}{\partial y}(x, y) \to \frac{3}{2}\frac{\sin x}{x},\ \theta(x, y) \to 0 \quad \text{as} \quad y \to \infty,\ 0 \le x \le \pi \tag{10}$$

It can be seen that near the lower stagnation point of the sphere, i.e. $x \approx 0$, (8) and (9) reduce to the following ordinary differential equations:

$$\frac{1}{(1-\varphi)^{2.5}} f' = \frac{3}{2}\frac{1}{(1-\varphi)^{2.5}} + \left[1-\varphi+\varphi\left(\rho_s/\rho_f\right)\left(\beta_s/\beta_f\right)\right]\lambda\theta, \tag{11}$$

$$\frac{k_{nf}/k_f}{(1-\varphi)+\varphi\left(\rho C_p\right)_s/\left(\rho C_p\right)_f}\theta'' + f\theta' = 0, \tag{12}$$

with the boundary conditions:

$$f(0) = 0,\ \theta(0) = 1,\ f'(y) \to \frac{3}{2},\ \ \theta(y) \to 0 \ \text{ as } \ y \to \infty \tag{13}$$

where primes denote differentiation with respect to y. Quantity of practical interest is the skin friction coefficient C_f, which is defined as:

$$C_f = \frac{\tau_w}{\rho_f U_\infty^2}, \tag{14}$$

where τ_w is the surface shear stress, which is given by:

$$\tau_w = \mu_{nf}\left(\frac{\partial \bar{u}}{\partial \bar{y}}\right)_{\bar{y}=0}. \tag{15}$$

Substituting variables (7) into (14) and (15), we obtain,

$$(\mathrm{Pr}Pe^{1/2})C_f = \frac{x}{(1-\varphi)^{2.5}}\frac{\partial^2 f}{\partial y^2}(x,0). \tag{16}$$

Results and Discussion

Equations (8) and (9), subject to the boundary conditions (10) have been solved numerically using an efficient implicit finite-difference scheme known as the Keller-box method along with the Newton's linearization technique as described by Cebeci and Bradshaw (1988). Three different types of nanoparticles, namely Cu, Al_2O_3 and TiO_2 (with water as their base fluid), have been considered in this study and representative results for the skin friction coefficient, $(\mathrm{Pr}Pe^{1/2})C_f$, have been obtained for the following range of nanoparticle volume fraction φ: $\varphi = 0$, 0.1 and 0.2 (Abu-Nada & Oztop 2009), at different positions x with various values of the mixed convection parameter λ. The numerical solution starts at the lower stagnation point of the sphere, $x \approx 0$ and proceeds round the sphere up to the separation point. The present results are obtained up to $x = 120^o$ only. We have used data related to thermophysical properties of the fluid and nanoparticles as given in Oztop and Abu-Nada (2008) to compute each case of the nanofluid.

Tables 1 and 2 show the values of $(\mathrm{Pr}Pe^{1/2})C_f$ for φ = 0.1 and 0.2 for nanoparticles Cu at different positions x and various values of the mixed convection parameter λ, respectively. It is observed from these tables that the skin friction coefficients $(\mathrm{Pr}Pe^{1/2})C_f$ are negative when $\lambda > 0$ and positive when $\lambda < 0$ and zero when $\lambda = 0$ due to the definition of $(\mathrm{Pr}Pe^{1/2})C_f$ given in (16). It is found that for fixed x and λ, as the value of the nanoparticle volume fraction φ increases from 0 to 0.2, it results in an increase in the value of the location of the separation point and a decrease in the magnitude of the skin friction coefficient $(\mathrm{Pr}Pe^{1/2})C_f$ and this applies in both the heated sphere ($\lambda > 0$) and the cooled sphere ($\lambda < 0$) cases.

It is observed from Tables 1 and 2 for the case of the nanoparticles Cu that the actual value of $\lambda = \lambda_s\ (>0)$ which first gives no separation of boundary layer is difficult to determine exactly as it has to be found by successive integration of the equations. However, the numerical solutions indicate that the value of λ_s which first gives no separation lies between -2.09 and -2.10 for $\varphi = 0.1$ and between -2.89 and -2.90 for $\varphi = 0.2$. Meanwhile the value (negative) of $\lambda = \lambda_0\ (< 0)$ below which a boundary layer separation is not possible for nanoparticles Cu, are -2.46 for $\varphi = 0.1$ and -3.3 for $\varphi = 0.2$. The same trend can be observed for the cases of nanoparticles Al_2O_3 and TiO_2. It is found that the boundary layer starts to separate the fastest (with highest values of $\lambda_s\ (>0)$) for the nanoparticles Cu, followed by Al_2O_3 and TiO_2. This indicates that the nanoparticles TiO_2 delay the start of the boundary layer separation from the sphere.

Figures 1 and 2 show the skin friction coefficient $(\mathrm{Pr}Pe^{1/2})C_f$ for $\lambda = 1$ (assisting flow) and $\lambda = -1$ (opposing flow), respectively, with various values of $\varphi = 0.0$ (regular Newtonian fluid), 0.1 and 0.2, for the three nanoparticles considered, namely Cu, Al_2O_3 and TiO_2. It is seen from these figures that due to the definition of $(\mathrm{Pr}Pe^{1/2})C_f$, the skin friction coefficients are negative when $\lambda > 0$ (assisting flow) and positive when $\lambda < 0$ (opposing flow). The negative values of the skin friction coefficient from Figure 1 corresponds to the surface exerts a drag force on the fluid and the positive values from Figure 2 implies the opposite. On the other hand, the parabolic shape of the curves in Figure 1 for the case of $\lambda = 1$ (assisting flow) implies that the skin friction coefficient is zero at the lower stagnation point of the sphere, $x \approx 0$ and as we proceed round the sphere, the skin friction coefficient decreases to its minimum value at around halfway up to the separation point. Beyond this point, the skin friction coefficient increases to a finite value at $x = 120^o$. The opposite trends are observed when $\lambda = -1$ (opposing flow) as shown in Figure 2 with the parabolic curve having a maximum value. These phenomena are observed for the skin friction coefficient curves involving a sphere or a circular cylinder. It is possibly due to the shapes of sphere and circular cylinder which consequently lead to flow separation. It is also observed from these figures that the magnitude of the skin friction coefficient decreases as φ increases from 0 to 0.2. Also it is seen that the magnitude of the skin friction

TABLE 1. Values of the skin friction coefficient ($PrPe^{1/2}$) C_f for Cu nanoparticles when $\varphi = 0.1$ and various values of λ

							λ					
x	- 2.46	- 2.22	- 2.13	- 2.10	- 2.09	- 2.0	- 1.0	- 0.5	0.5	1.0	2.0	5.0
0°	0.0000	0.0000	0.0000	0.0000	0.0000	0.0000	0.0000	0.0000	-0.0000	-0.0000	-0.0000	-0.0000
10°	0.2096	0.2308	0.2341	0.2347	0.2349	0.2355	0.1643	0.0913	-0.1071	-0.2283	-1.5932	-0.5081
20°		0.4474	0.4537	0.4550	0.4553	0.4566	0.3184	0.1770	-0.2077	-0.4426	-3.0885	-0.9850
30°		0.6369	0.6460	0.6478	0.6482	0.6500	0.4533	0.2520	-0.2956	-0.6301	-4.3966	-1.4022
40°		0.7877	0.7995	0.8017	0.8023	0.8046	0.5611	0.3119	-0.3659	-0.7800	-5.4420	-1.7356
50°			0.9061	0.9087	0.9093	0.9119	0.6360	0.3535	-0.4148	-0.8840	-6.1681	-1.9672
60°			0.9609	0.9636	0.9644	0.9671	0.6746	0.3749	-0.4399	-0.9376	-6.5417	-2.0864
70°			0.9629	0.9657	0.9664	0.9692	0.6762	0.3758	-0.4409	-0.9397	-6.5559	-2.0911
80°			0.9135	0.9178	0.9185	0.9213	0.6429	0.3573	-0.4191	-0.8932	-6.2311	-1.9876
90°				0.8268	0.8275	0.8302	0.5795	0.3220	-0.3776	-0.8049	-5.6138	-1.7908
100°				0.7026	0.7037	0.7064	0.4931	0.2739	-0.3212	-0.6846	-4.7738	-1.5230
110°				0.5541	0.5606	0.5631	0.3928	0.2182	-0.2557	-0.5450	-3.7994	-1.2123
120°					0.4172	0.4158	0.2888	0.1604	-0.1879	-0.4004	-2.7901	-0.8905

TABLE 2. Values of the skin friction coefficient ($PrPe^{1/2}$) C_f for Cu nanoparticles when $\varphi = 0.2$ and various values of λ

							λ					
x	- 3.30	-3.07	- 2.94	- 2.90	- 2.89	- 2.0	- 1.0	- 0.5	0.5	1.0	2.0	5.0
0°	0.0000	0.0000	0.0000	0.0000	0.0000	0.0000	0.0000	0.0000	-0.0000	-0.0000	-0.0000	-0.0000
10°	0.2541	0.2683	0.2721	0.2728	0.2730	0.2448	0.1467	0.0787	-0.0883	-0.1853	-0.4034	-1.2207
20°		0.5201	0.5275	0.5289	0.5292	0.4745	0.2844	0.1525	-0.1711	-0.3593	-0.7821	-2.3663
30°		0.7404	0.7510	0.7530	0.7533	0.6755	0.4049	0.2171	-0.2436	-0.5115	-1.1134	-3.3686
40°		0.9145	0.9296	0.9320	0.9325	0.8362	0.5012	0.2687	-0.3015	-0.6331	-1.3781	-4.1696
50°			1.0536	1.0563	1.0569	0.9478	0.5681	0.3046	-0.3417	-0.7176	-1.5620	-4.7259
60°			1.1175	1.1203	1.1209	1.0054	0.6026	0.3231	-0.3625	-0.7611	-1.6567	-5.0122
70°			1.1201	1.1229	1.1234	1.0079	0.6040	0.3238	-0.3633	-0.7628	-1.6604	-5.0232
80°			1.0656	1.0674	1.0680	0.9583	0.5742	0.3079	-0.3453	-0.7251	-1.5782	-4.7745
90°				0.9621	0.9627	0.8634	0.5175	0.2774	-0.3112	-0.6533	-1.4220	-4.3015
100°				0.8189	0.8197	0.7341	0.4403	0.2360	-0.2647	-0.5557	-1.2094	-3.6580
110°				0.6515	0.6551	0.5843	0.3507	0.1880	-0.2107	-0.4424	-0.9628	-2.9116
120°					0.4915	0.4293	0.2579	0.1381	-0.1548	-0.3250	-0.7072	-2.1383

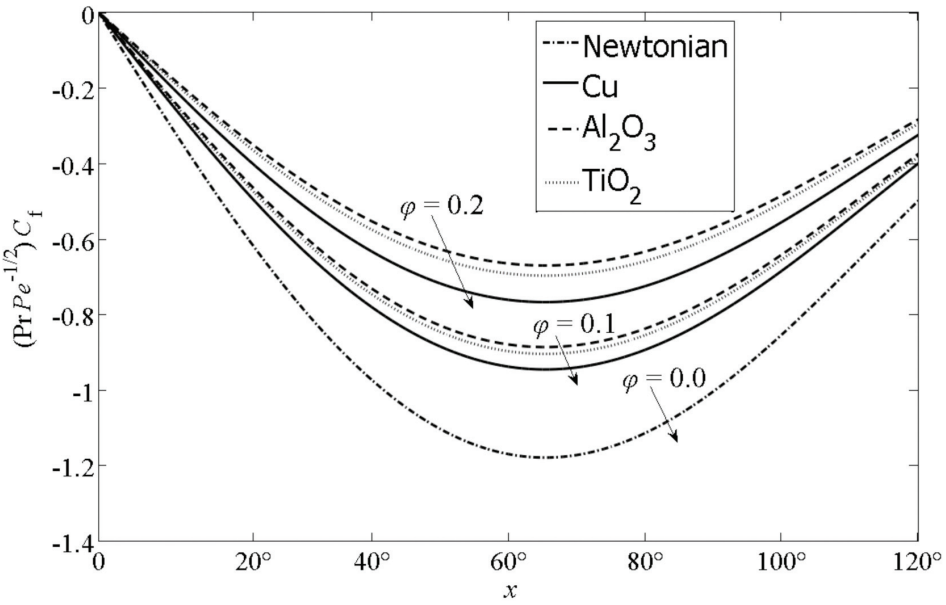

FIGURE 1. Comparison of the skin friction coefficient $(\mathrm{Pr}Pe^{1/2})C_f$ when $\lambda = 1$ (assisting flow) for various nanoparticles and various values of φ (φ = 0.0, 0.1 and 0.2)

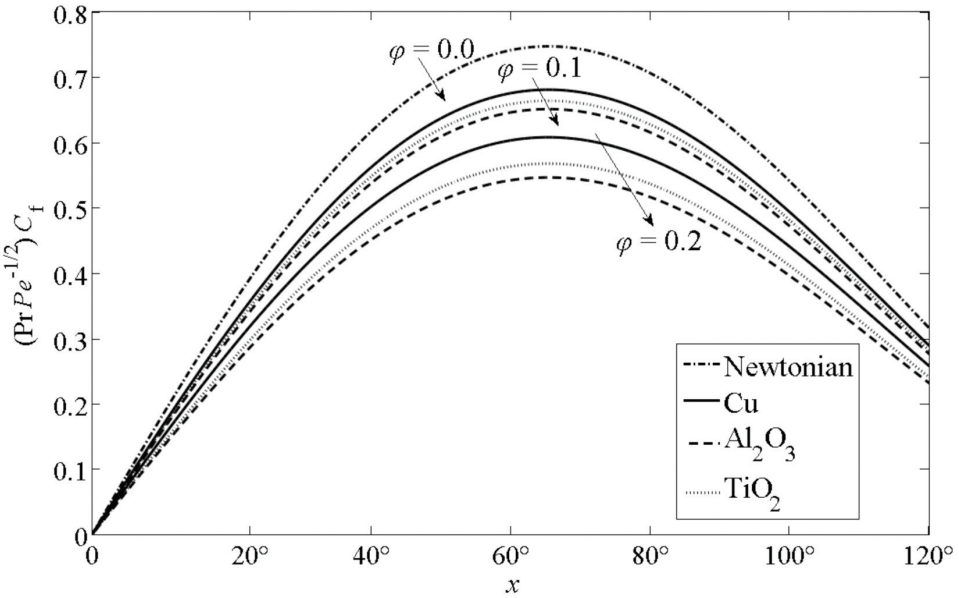

FIGURE 2. Comparison of the skin friction coefficient $(\mathrm{Pr}Pe^{1/2})C_f$ when $\lambda = -1$ (opposing flow) for various nanoparticles and various values of φ (φ = 0.0, 0.1 and 0.2)

coefficient for the regular fluid is higher than the nanofluid. Among the three nanoparticles, the magnitude of the skin friction coefficient is the highest for Cu (nanoparticles with high density and thermal diffusivity), followed by TiO_2 and the lowest is Al_2O_3 (nanoparticles with low thermal diffusivity). It should be pointed out that nanofluids have lower skin friction coefficient compared with the base fluid, which is good to be used as lubricant, due to the suspended nanoparticles that can stay longer in the base fluid and the surface area per unit volume of nanoparticles is large. These two properties can enhance the flow characteristic of nanofluids.

Figure 3 shows the velocity profiles, $f'(y)$, at the lower stagnation point of the sphere, $x \approx 0$, of nanoparticles Cu, when $\lambda = 1, 2$ (assisting flow) and $\lambda = -1$ (opposing flow), with the nanoparticle volume fraction $\varphi = 0.0$, 0.1 and 0.2. It is clear that, as the nanoparticles volume fraction increases, the nanofluid velocity decreases, however, the opposite results are observed at $\lambda = -1$. Figure 4 shows the temperature profiles, $\theta(y)$, at the lower stagnation point of the sphere, $x \approx 0$, for nanoparticles Cu, when $\lambda = 1, 2$ (assisting flow) and $\lambda = -1$ (opposing flow), with the nanoparticle volume fraction $\varphi = 0.0$, 0.1 and 0.2. This figure illustrates this agreement with the physical

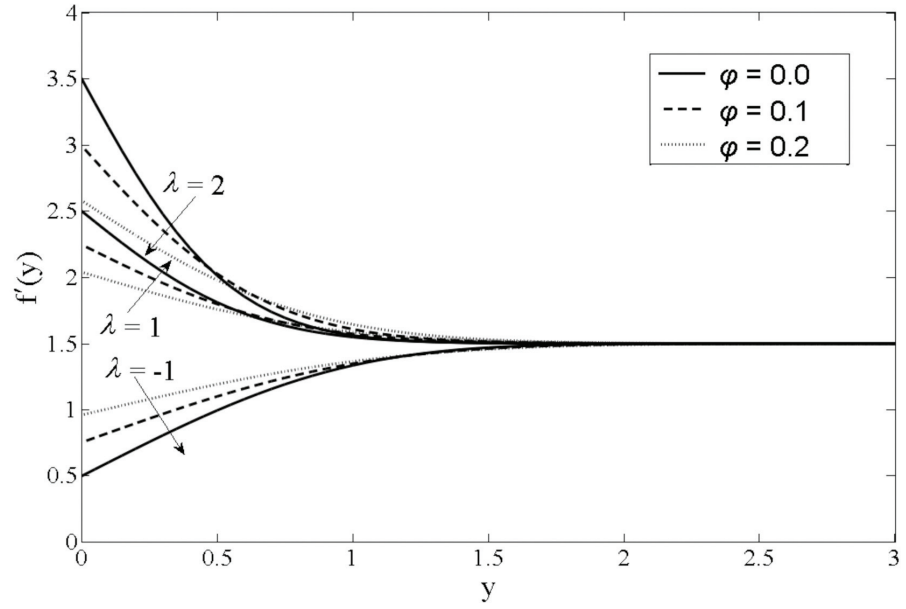

FIGURE 3. Velocity profiles $f'(y)$ at the lower stagnation point of the sphere, $x \approx 0$, for Cu nanoparticles with φ = 0.0, 0.1 and 0.2 and various values of λ ($\lambda = 2$, $\lambda = 1$ and $\lambda = -1$)

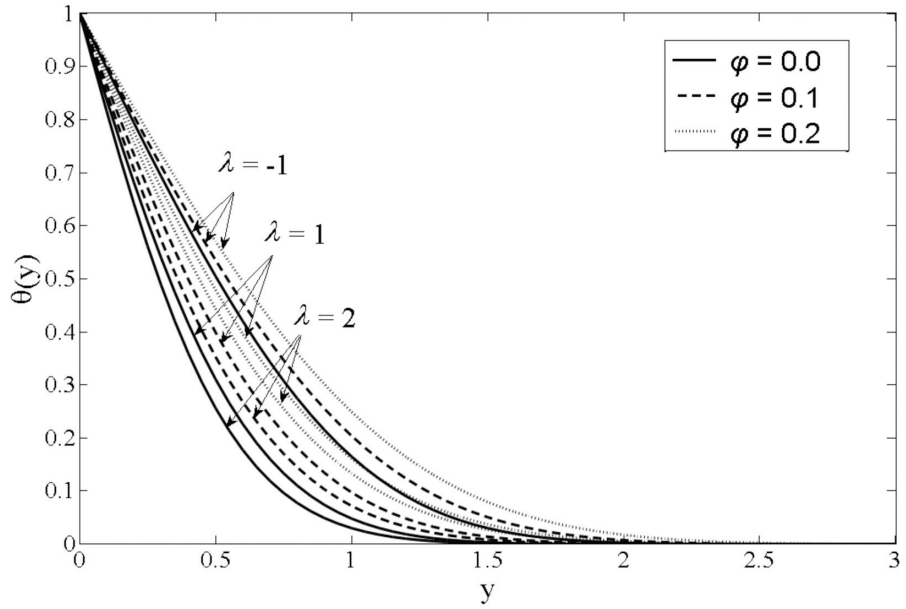

FIGURE 4. Temperature profiles $\theta(y)$ at the lower stagnation point of the sphere, $x \approx 0$, for Cu nanoparticles with φ = 0.0, 0.1 and 0.2 and various values of λ ($\lambda = 2$, $\lambda = 1$ and $\lambda = -1$)

behavior, that is, when the volume of nanoparticles increases, the thermal conductivity increases and then the thermal boundary layer thickness increases. This is due to the presence of the nanoparticles in the fluids increases appreciably the effective thermal conductivity of the fluid and consequently enhances the heat transfer characteristics (Hady et al. 2012). From all the velocity and temperature profiles, it is observed that the profiles satisfy the far field boundary conditions asymptotically, and as such, this support the validity of the numerical results obtained.

CONCLUSION

In this paper, we have studied the problem of steady laminar mixed convection flow over an isothermal sphere embedded in a porous medium filled with a nanofluid. We have looked into the effects of the mixed convection parameter λ, the type of nanoparticles (Al_2O_3, Cu, TiO_2) and the nanoparticle volume fraction φ on the flow and heat transfer characteristics. The governing non-similar boundary layer equations were solved numerically using the Keller-box method. From this study, we could draw the following conclusions: an increase in the value of φ led to a

decrease in the skin friction coefficient, $(\mathrm{Pr}Pe^{1/2})C_f$, and to an increase in the value of $\lambda = \lambda_s\,(>0)$ which first gives no separation; an increase in the value of φ led to a decrease in the value of $\lambda = \lambda_0\,(<0)$ below which a boundary layer solution does not exist and the nanoparticles Cu has the highest value of the skin friction coefficient, $(\mathrm{Pr}Pe^{1/2})C_f$, compared with the nanoparticles TiO_2 and Al_2O_3. Besides that, it was found that the type of nanofluid was a key factor for heat transfer enhancement. The highest values were obtained when using the Cu nanoparticles.

ACKNOWLEDGEMENT

The authors would like to acknowledge the financial supports received in the form of the fundamental research grant scheme (FRGS) and LRGS/TD/2011/UKM/ICT/03/02 from the Ministry of Higher Education, Malaysia and UKM-OUP-FST-2012.

REFERENCES

Abu-Nada, E. 2008. Application of nanofluids for heat transfer enhancement of separated flows encountered in a backward facing step. *Int. J. Heat Fluid Flow* 29: 242-249.

Abu-Nada, E. & Oztop, H.F. 2009. Effects of inclination angle on natural convection in enclosures filled with Cu-water nanofluid. *Int. J. Heat Fluid Flow* 30(4): 669-678.

Ahmad, S. & Pop, I. 2010. Mixed convection boundary layer flow from a vertical flat plate embedded in a porous medium filled with nanofluids. *Int. Comm. Heat Mass Transfer* 37(8): 987-991.

Arifin, N.M., Nazar, R. & Pop, I. 2011. Viscous flow due to a permeable stretching/ shrinking sheet in a nanofluid. *Sains Malaysiana* 40: 1359-1367.

Bachok, N., Ishak, A., Nazar, R. & Pop, I. 2010. Flow and heat transfer at a general three-dimensional stagnation point in a nanofluid. *Physica B: Condensed Matter* 405(24): 4914-4918.

Brinkman, H.C. 1952. The viscosity of concentrated suspensions and solutions. *J. Chem. Phys.* 20: 571-581.

Buongiorno, J. 2006. Convective transport in nanofluids. *ASME J. Heat Transfer* 128(3): 240-250.

Cebeci, T. & Bradshaw, P. 1988. *Physical and Computational Aspects of Convective Heat Transfer.* New York: Springer.

Cheng, P. 1982. Mixed convection about a horizontal cylinder and a sphere in a fluid saturated porous medium. *Int. J. Heat Mass Transfer* 25: 1245-1247.

Choi, S.U.S. 1995. Enhancing thermal conductivity of fluids with nanoparticles. In *Development and applications of non-Newtonian Flows*. D.A. Siginer & H.P. Wang (eds.). *ASME MD-vol. 231 and FED-vol.* 66: 99-105.

Das, S.K., Choi, S.U.S., Yu, W. & Pradet, T. 2007. *Nanofluids: Science and Technology*. New York: Wiley.

Daungthongsuk, W. & Wongwises, S. 2008. Effect of thermophysical properties models on the predicting of the convective heat transfer coefficient for low concentration nanofluid. *Int. Comm. Heat Mass Transfer* 35: 1320-1326.

Eastman, J.A., Choi, S.U.S., Li, S., Yu, W. & Thompson, L.J. 2010. Anomalously increased effective thermal conductivity of ethylene glycol-based nanofluids containing copper nanoparticles. *J. Appl. Phys. Lett.* 78(6): 718-720.

Hady, F.M., Ibrahim, F.S., Abdel-Gaied, S.M. & Eid, M.R. 2012. Radiation effect on viscous flow of a nanofluid and heat transfer over a nonlinearly stretching sheet. *Nanoscale Research Letters* 7: 229(1-13).

Jou, R.Y. & Tzeng, S.C. 2006. Numerical research of nature convective heat transfer enhancement filled with nanofluids in rectangular enclosures. *Int. Comm. Heat Mass Transfer* 33(6): 727-736.

Kang, H.U., Kim, S.H. & Oh, J.M. 2006. Estimation of thermal conductivity of nanofluid using experimental effective particle volume. *Exp. Heat Transfer* 19: 181-191.

Khanafer, K., Vafai, K. & Lightstone, M. 2003. Buoyancy-driven heat transfer enhancement in a two-dimensional enclosure utilizing nanofluids. *Int. J. Heat Mass Transfer* 46(19): 3639-3653.

Kumar, S., Prasad, S.K. & Banerjee, J. 2010. Analysis of flow and thermal field in nanofluid using a single phase thermal dispersion model. *Appl. Math. Modelling* 34(3): 573-592.

Merkin, J.H. 1977. Mixed convection from a horizontal circular cylinder. *Int. J. Heat Mass Transfer* 20: 73-77.

Nazar, R., Amin, N. & Pop, I. 2003. The Brinkman model for the mixed convection boundary layer flow past a horizontal circular cylinder in a porous medium. *Int. J. Heat Mass Transfer* 46(17): 3167-3178.

Nazar, R., Tham, L., Pop, I. & Ingham, D.B. 2011. Mixed convection boundary layer flow from a horizontal circular cylinder embedded in a porous medium filled with a nanofluid. *Trans. Porous Media* 86: 517-536.

Nield, D.A. & Bejan, A. 2006. *Convection in Porous Media*. New York: Springer.

Oztop, H.F. & Abu-Nada, E. 2008. Numerical study of natural convection in partially heated rectangular enclosures filled with nanofluids. *Int. J. Heat Fluid Flow* 29(5): 1326-1336.

Rosca, N.C., Grosan, T. & Pop, I. 2012. Stagnation-point flow and mass transfer with chemical reaction past a permeable stretching sheet in a nanofluid. *Sains Malaysiana* 41(10): 1271-1279.

Tiwari, R.K. & Das, M.K. 2007. Heat transfer augmentation in a two-sided lid-driven differentially heated square cavity utilizing nanofluids. *Int. J. Heat Mass Transfer* 50(9-10): 2002-2018.

Leony Tham
Fakulti Industri dan Asas Tani
Universiti Malaysia Kelantan
17600 Jeli, Kelantan
Malaysia

Roslindar Nazar*
Pusat Pengajian Sains Matematik
Fakulti Sains dan Teknologi
Universiti Kebangsaan Malaysia
43600 UKM Bangi, Selangor
Malaysia

*Corresponding author; email: rmn@ukm.my

Received: 18 May 2012
Accepted: 31 July 2012